

4118304669

KFKI-1982-106

Y. ALPERT,  
L. CSER,  
B. FARAGÓ,  
F. FRANEK,  
F. MEZEI,  
YU.M. OSTANEVICH

FLEXIBILITY AND CONFORMATIONAL CHANGE  
OF IgG MOLECULE

*Hungarian Academy of Sciences*

**CENTRAL  
RESEARCH  
INSTITUTE FOR  
PHYSICS**

**BUDAPEST**

FLEXIBILITY AND CONFORMATIONAL CHANGE  
OF IgG MOLECULE

Y. Alpert\*, L. Cser, B. Faragó, F. Franek\*\*,  
F. Mezei\*\*\*, Yu.M. Oostanevich\*\*\*\*

Central Research Institute for Physics  
H-1525 Budapest 114, P.O.B.49, Hungary

\*Institut de Biologie Physico-Chimique  
13 Rue Pierre et Marie Curie 75005, Paris

\*\*Institute of Molecular Genetics  
Czechoslovak Academy of Sciences, Prague

\*\*\*Institut Laue-Langevin,  
156X Centre de Tri  
38042 Grenoble Cedex, France

\*\*\*\*Laboratory of Neutron Physics  
JINR, Dubna, USSR

*Submitted to European Journal of Biochemistry*

## ABSTRACT

The dynamic behaviour of pig anti-Dnp-immunoglobulin (IgG) investigated by the neutron spin echo technique gave evidence of internal motion of a biological macromolecule. It is suggested that this motion belongs to the wobbling of the Fab parts of the investigated IgG molecule around its so called hinge region.

## АННОТАЦИЯ

С помощью метода нейтронного спинового эха исследовано динамическое поведение молекулы анти-Dnp-иммуноглобулина (IgG) свиней. Показано существование внутреннего движения исследованной макромолекулы, что связано со случайным блуждающим вращением Fab частей молекулы вокруг связывающего их с Fc частью "шарнирным" участком пептидной цепи.

## KIVONAT

Sertés anti-Dnp-immunoglobulin (IgG) dinamikáját vizsgáltuk neutron spin echoval. Első ízben sikerült belső mozgást megfigyelni biológiai makromolekulán. A megfigyelt mozgás jól leírható az IgG Fab részeinek a kapcsolódási pont körüli elfordulásával.

## INTRODUCTION

The structure of IgG type immunoglobulin molecules has widely been investigated [1] and it appears that the amino-acid sequence in the IgG molecule is loosely packed. The molecule consists of three weakly connected distinct parts: two of which (so called Fab) are elongated, while the shape of the third one (Fc-part) is more sophisticated, having a hole in its middle region [2]. As a whole, the IgG molecule has either a T-shaped or, so called shirt-shaped form [3]. It is thought that the shape of the IgG molecule has a meaning related to time average only, and various types of intensive internal motion (wagging and twisting of the three parts, or conformational motion of the amino acid chain) were assumed.

This raises two crucial questions: first, what is the dominant type of motion? Second, does the internal motion of the IgG molecule play an important role in its function?

In an attempt to answer these questions, the nanosecond fluorescence polarization technique was recently applied [4,5]. In these experiments fluorescent chromophore  $\epsilon$ -dansyl-L-lysine groups were specifically bound to the binding sites of antidansyl antibody, and the emission anisotropy of the bound dansyl group was measured as a function of time following excitation by a nanosecond light pulse. The decay of the initial polarization value may be due to the rotation of the dansyl group itself but also to the wagging and wobbling of the Fab parts and to the rotational diffusion of the IgG molecule as a whole. The results above indicated that the decay of fluorescence anisotropy involved two rotational correlation times: the long correlation time corresponding to the global tumbling of the molecule, the shorter one representing a flexible motion of the Fab parts [4]. However, this interpretation has been somewhat revised [5], viz. the longer correlation time is said to be related to the wagging and wobbling motions of Fab parts, with the shorter one representing either the flexibility of the variable domains of the molecule around the hinge region of the constant and variable domains' peptide chains or the twisting of the Fab part around its long axis.

The flexibility properties of IgG molecules could better be elucidated using neutron scattering which provides information not only on the time dependence but also on the momentum dependence of the process. This would give space - time information on the motion of the arms. In the simplest approach the flexibility should show up in the  $\chi$ -dependence of the effective diffusion constant defined as the ratio of the inelastic linewidth  $\Gamma$  to the square of the momentum transfer  $\chi$  :  $D_{\text{eff}} = \Gamma/\chi^2$ . In the  $\chi = 0$  limit,  $D_{\text{eff}}$  should be equal to the macroscopic translational diffusion constant  $D_{\text{tr}}$ .

The resolution required in this type of measurement should be of the order of nanoeV, and the momentum transfer less than  $2 \text{ nm}^{-1}$ .

These requirements may be satisfied by the possibilities of the neutron spin-echo spectrometer installed at ILL's high-flux reactor.

## MATERIALS AND METHODS

Antibodies to dinitrophenyl (Dnp) were isolated from sera of pigs immunized by dinitrophenylated bovine immunoglobulin [6,7]. Precipitating antibody was isolated from sera collected at an early phase of the immune response [8,9]. This antibody belongs to the IgG immunoglobulin class ( $M = 150\ 000$ ). The preparations used in the present work were the same as those used earlier [10].

Neutron scattering was performed on samples of 7.36 w.% and 3.68 w.% antibody dissolved in 0.1 M NaCl sodium phosphate heavy water buffer, adjusted to pH = 6.6 and on a 7.36 w.% solution to which 18 w.% sucrose was added.

The antibody solutions were equilibrated by dialysis against the relevant buffer. Possible aggregates were removed from the solutions by centrifuging at 6000g for 20 min.

In these experiments we used a 6 mm thick cell made of optical quartz. The sample temperature was stabilized at  $14^\circ\text{C}$ .

The neutron scattering experiment was carried out on the neutron spin-echo spectrometer (IN11) at the ILL [11,12]; this spectrometer has an energy resolution of about 1 neV at  $\lambda = 8.4 \text{ \AA}$  neutron wavelength.

The spin-echo spectra were evaluated using a deuterated polystyrene solid sample as standard elastic scatterer for calibration [12], that gave a similar small angle scattering pattern to the investigated samples.

In addition, we determined the viscosity of the solutions by a capillary viscosimeter.

## EXPERIMENTAL RESULTS

At low  $\chi$  values the neutron spin echo signal as a function of time was found to correspond within the statistical accuracy to the pure exponential decay  $\exp(-\Gamma t)$  characterizing the Lorentzian lineshape [11]. At high  $\chi$  values, however, there were signs of deviations (see Fig. 1) and the superposition of two or more exponential functions seemed to give a better description.

Since this deviation was not too pronounced, we determined  $\Gamma$  by least squares fitting the spectra to a single exponential form.

From the obtained  $\Gamma$  values we evaluated the effective diffusion constant defined as the ratio of  $\Gamma$  and the square of the momentum transfer  $\chi$ :

$$D_{\text{eff}} = \Gamma / \chi^2.$$

These  $D_{\text{eff}}$  values are given in Fig. 2 for different solutions as a function of the momentum transfer. Unfortunately the  $\chi \rightarrow 0$  limit of  $D_{\text{eff}}$ , the macroscopic translation diffusion constant  $D_{\text{tr}}$ , is poorly known. The  $\chi$  range from which  $D_{\text{tr}}$  may be determined from neutron inelastic scattering data is less than  $\chi_0 = 1/R_g$ . As can be seen from Fig. 2 the accuracy and resolution of the present experiment were inadequate for determining the  $D_{\text{tr}}$  value.

However, recent data, obtained for non specific immunoglobulins in  $\text{H}_2\text{O}$  and extrapolated to zero concentration [13] permit one to estimate the diffusion data for the given solutions, using the results of our viscosity measurements. These  $D_{\text{tr}}$  values shown by the arrows in Fig. 2 are below the observed  $D_{\text{eff}}$  values. The only exception is the set of the points belonging to the solution containing sucrose. In this case all measured points correspond within the experimental error to the value of  $D_{\text{tr}}$ .

At increasing  $\chi$  values one can observe a slightly pronounced maximum in the  $D_{\text{eff}}$  versus  $\chi$  plot, beyond which the  $D_{\text{eff}}$  values tend to decrease with increasing  $\chi$ .

## DISCUSSION

For quantitative estimation of experimental data two types of model were constructed.

- 1.) The molecule has a rigid T-shaped form (rigid model) and the only permitted motion, - apart from the translational diffusion - is the rotational diffusion of the global molecule.

- 2.) A wagging or conelike wobbling motion of the Fab arms around the hinge region should be considered (flexible model). With this model the motion of the Fc part was neglected. We supposed that the Fc part - having a

more compact shape than the Fab ones [2] and being inserted between them [3] - could not move so much as the Fab arms, consequently it gives a much smaller contribution to the inelastic scattering intensity.

For both models the Fab parts were constructed from two prolate ellipsoids of revolution connected at the end points of their longer axes. Both the total length and the thickness of the Fab arms were changeable parameters. The Fc part was also represented by an ellipsoid of revolution whose volume was equal to the volume of the Fab arm.

The corresponding scattered intensity distributions were computed using the following formula (for detailed deduction, see Appendix):

$$|I(X,t) = e^{-D_{tr} X^2 t} \sum_{\ell} (2\ell+1) [2 \cdot A_{\ell}^{(0)}(X)^2 (1+(-1)^{\ell}) + 4A_{\ell}^{(0)}(X) A_{\ell}^{(1)}(X) P_{\ell}(0) + A_{\ell}^{(1)}(X)^2] \cdot \exp(-\ell(\ell+1) D_r^T t) \quad (1a)$$

for the rigid model and

$$|I(X,t) = e^{-D_{tr} X^2 t} \sum_{\ell} (2\ell+1) [2 \cdot A_{\ell}^{(0)}(X)^2 \{ (1 - \langle P_{\ell}(\cos\beta) \rangle^2) \cdot \exp(-\ell(\ell+1) D_r^T t) + (1+(-1)^{\ell}) \langle P_{\ell}(\cos\beta) \rangle^2 \} + 4A_{\ell}^{(0)}(X) A_{\ell}^{(1)}(X) \langle P_{\ell}(\cos\beta) \rangle P_{\ell}(0) + A_{\ell}^{(1)}(X)^2] \quad (1b)$$

for the flexible model.

Here we used the following notations:

$$A_{\ell}^{(i)}(X) = \int_0^a J_{\ell}(Xr) \rho^{(i)}(r) r^2 dr$$

(i=0 for Fab region, i=1 for Fc region);  $J_{\ell}(Xr)$  is the  $\ell$ -th spherical Bessel function;

$$\rho_{\ell}^{(i)}(r) = \sqrt{\frac{4\pi}{2\ell+1}} \rho_{\ell 0}^i(r)$$

is the  $\ell$ -th term of the density distribution of the Fab (i=0) and Fc (i=1) parts expanded by the spherical harmonics;  $\langle P_{\ell}(\cos\beta) \rangle$  is the  $\ell$ -th order Legendre polynomial averaged over a cone inside which the Fab arm could be oriented randomly with uniform probability. The cone is characterized by the value of  $\beta_{\max}$  which gives the maximum tilting angle of the Fab arm with respect to its average value;  $a$  - is the total length of the Fab arm;  $D_r^T$  - is the rotational diffusion coefficient of the whole molecule;  $D_r$  - is the

rotational diffusion coefficient of one Fab arm around the hinge region. The  $I(\chi, t)$  functions were evaluated using the above formula at fixed  $\chi$ , and at different  $t$  values, then these were estimated by exponential functions  $\exp(-D_{\text{eff}}^{(c)} \chi^2 t)$  in the same way as in the experiment. The  $D_{\text{eff}}^{(c)}(\chi) - D_{\text{tr}}$  curves were compared with the measured  $D_{\text{eff}} - D_{\text{tr}}$  experimental points (see Fig. 3).

As was mentioned earlier,  $D_{\text{tr}}$  values were estimated from data obtained for human IgG. However, other hydrodynamic data, viz. the values of sedimentation constants for different human and for our pig IgG differ by no more than 3-5%, consequently the difference between the corresponding diffusional constants should be of the same order. It means that our estimation of  $D_{\text{tr}}$  values is quite accurate.

The model calculations were restricted to the solution of 7.33 w.% since these data are the most accurate and were obtained over a wide  $\chi$  range.

As may be seen from Fig. 3 all three calculated curves give rise to the estimation of experimental points more or less accurately, and to make a choice between them on the basis of shape alone is almost impossible.

But there are several items of auxiliary information which help us to decide which model is best able to describe the real situation.

Let us first consider the rigid model. To achieve a good approximation in this case we were forced to choose the value of the rotational diffusion coefficient  $D_r^T = 1/1700 \text{ nsec}^{-1}$  or, what is equivalent, to choose the corresponding correlation time  $\tau_T = 1/D_r^T = 1700 \text{ nsec}$  (see Table I).

A body having anisotropic shape possesses several rotational diffusion coefficients. Namely, a prolate ellipsoid of revolution has two rotational diffusion coefficients  $D_{\perp}$  and  $D_{\parallel}$ .  $D_{\perp}$  and  $D_{\parallel}$  are the coefficients for rotational diffusion around the major and minor axes, of the ellipsoid, respectively.

The shape of the IgG molecule in first approximation may be estimated by an equivalent ellipsoid of revolution since its length (i.e. the distance between the tips of the Fab arms) is about three times greater than the height of the Fc part and about five times greater than the thickness of the molecule. Moreover, from symmetric considerations it follows that the main contribution to the form-factor arising in the inelastic neutron scattering cross-section comes from the rotation around the short axes and only a small contribution arises from the rotation around the longest one.

The ratio of  $D_{\perp}$  to the rotational diffusion coefficient  $D$  of a sphere of equal volume may be calculated from the ratio of the length of the major and minor axes [4]. The  $D$  value we estimated through the hydrodynamic radius

( $R_H$ ) obtained from the Stokes-Einstein equation [14] giving a value  $R_H = 5.54$  nm. Choosing for the ratio of major and minor axes a value of 3.5 which is quite realistic and using the formula [5]

$$D = \frac{kT}{8\pi\eta R_H^3} \quad (2)$$

we obtained  $\tau_r = 1/D_r^T = 6000$  nsec. This figure is much higher than came from the corresponding model computation and this big discrepancy cannot be explained by the roughness of our initial suppositions which were made performing this estimation. On the basis of this consideration we could not accept the rigid model as a realistic one.

At the same time, there are several arguments supporting the flexible model with  $\beta_{\max} = 50^\circ$ . Firstly, a recent observation by Valentine and Green [15] using an electronmicroscope shows that the deviation of Fab arms from the T-shaped form may achieve a value of  $60^\circ$ . Secondly, the correlation time of the wobbling-type motion of Fab arms obtained from our model is very close to that interpreted as a wobbling correlation time on the basis of the nanosecond fluorescence polarization technique [5] (see Table III). As a third argument we mentioned that the mean angle  $\bar{\beta}$  transversed by the Fab arms is  $24^\circ$ , which value is again very close to the  $\bar{\beta} = 33^\circ$  obtained by Yguerabide [4].

The fact that the maximum value of  $D_{\text{eff}}^{-D_{\text{tr}}}$  appears in the vicinity of  $\chi_1$ , which corresponds to the cross-section of the two straight-line parts of the small angle scattering intensity distribution given in the so called Porod coordinates [1] (see insert to Fig. 2), also indicates that the motion mainly belongs to the Fab parts of the immunoglobulin molecule since - as was shown earlier [1] -, above this  $\chi_1$  value the main contribution to the small angle scattering intensity came from the Fab part of the molecule.

The relatively small deviations between our data and the cited data may arise from our simplifying supposition that the probability of any deviation of Fab arms inside a given cone is uniform. It is more realistic to expect that the probability decreases when the angle of deviation increases. However, at this moment we do not possess any information about this probability.

Finally, despite the very small number of experimental points belonging to the solution with sucrose, the fact that  $D_{\text{eff}}$  in this case does not exhibit any  $\chi$ -dependence is of great importance. This effect means that in sucrose the additional motion either disappeared or becomes frozen-in, since a simple change of the viscosity could change only to an equal extent both the translational and rotational diffusion.

Unfortunately we have no idea of the true nature of this phenomenon, we suspect only that the added amount of sucrose appreciably changes the hydration shell of IgG molecules which, being polyampholite, get more strained if the screening of charged groups by the hydration water decreases. This decrease may arise since sucrose possesses many charged groups too.

In any case, measurement with sucrose demonstrates that for other solutions the additional motion observed at  $\lambda = 1/R_g$  belongs to the motion taking its origin from the flexibility of the IgG molecule.

Accepting the flexible model one should realize that the elastic small angle scattering data represent only the average shape of the IgG molecule since in the solution all allowed configurations exist simultaneously. Recently it was clearly shown that this intensity distribution corresponds to the T- or shirt-shaped form of the molecule [1], and the distance between the tips of the Fab arms was also determined [1].

The relatively intensive motion of the Fab arms may give rise to a shortening of the average distance ( $\bar{l}$ ) between the tips of the Fab arms and it is not obvious why the average shape of the molecule determined from the small angle scattering intensity distribution corresponds to models given in the cited papers.

To answer the first question we calculated the  $\bar{l}$  value as a function of  $\beta_{\max}$  using the Monte-Carlo method. The results given in Table III show that the shortening is not appreciable even in the case of  $\beta_{\max} = 50^\circ$ . The calculation of the average elastic small-angle scattering distribution in a similar way is much more complicated so we were restricted to qualitative considerations. First of all, the shortening of the  $\bar{l}$  value is small, since the weight of those motions of the Fab arms when they move to the opposite direction is not negligible and in this case the distance between the Fab tips remains almost unchanged. This type of qualitative argument could be used when the average shape is considered. As has been shown [1] the shirt-shaped model gives rise to a very similar small angle scattering pattern as does the T-shaped one. As a result, all those situations when both of the Fab arms are tilted to the Fc part do not alter the small angle scattering intensity distribution. Consequently, the probability of a Y-shaped conformation is appreciably reduced.

Secondly, as we suspect, the uniform probability of the deviation of Fab arms does not seem to be valid. A bell-shaped probability distribution reduces the accessible area of the deviation from the T-shaped form.

## CONCLUSIONS

During the course of our investigations we undoubtedly obtained the first neutron scattering evidence of internal motion of a biological macromolecule. This motion was identified as a wobbling type motion of the Fab arms of the investigated pig anti-Dnp-immunoglobulin. This interpretation is in accordance with the data of all other investigations. More extensive measurements would give rise to more detailed information of the observed internal motion.

Concerning the functional importance of the flexibility of the Fab arms we could only guess that a flexible molecule more easily finds and binds antigens than a rigid one.

## APPENDIX

From the general Van Hove formulae we can write the intermediate coherent scattering function

$$I(\chi, t) = \sum_{jj'} b_j^c b_{j'}^c \langle e^{-i\chi \hat{R}_j(0)} e^{i\chi \hat{R}_j(t)} \rangle \quad (\text{A.1})$$

where  $\hat{R}_j(t)$  is the position operator in the Heisenberg picture for the  $j$ -th nucleus at time  $t$ ;  $b_j^c$  is its scattering length. We are looking for different kinds of nearly macroscopic motions and so instead of the operators we can write simply the position vectors. In dilute solvents the interference between the molecules can be neglected, so we can sum up the scattering functions independently. Let us divide  $\underline{R}_j(t)$  into two parts

$$\underline{R}_j(t) = \underline{R}(t) + \underline{r}_j(t)$$

where  $\underline{R}(t)$  is the position of the centre of mass of the molecule;  $\underline{r}_j(t)$  stands for the position of the  $j$ -th nucleus with respect to it. One can assume that the diffusion of the centre of mass and the other motions, if any, are not coupled, then the averages can be performed separately, and in the case of simple diffusion [16], [17]

$$\begin{aligned} I(\chi, t) &= \langle e^{i\chi(\underline{R}(t) - \underline{R}(0))} \rangle \sum_{jj'} b_j^c b_{j'}^c \langle e^{-i\chi \underline{r}_j(t)} e^{i\chi \underline{r}_j(0)} \rangle \\ &= e^{-\chi^2 D t} \text{tr} \sum_{jj'} b_j^c b_{j'}^c \langle e^{-i\chi \underline{r}_j(t)} e^{i\chi \underline{r}_j(0)} \rangle \end{aligned} \quad (\text{A.2})$$

To evaluate the second part let us expand  $e^{i\chi r_j}$  into spherical harmonics, where  $r_j$  belongs to one of the fragments;

$$e^{i\chi r_j} = \sum_{\ell=0}^{\infty} \sqrt{4\pi(2\ell+1)} \varphi_{\ell 0}(\theta, \phi) j_{\ell}(\chi r_j) i^{\ell} \quad (A.3)$$

In this coordinate system (space system) the z axis is chosen to be parallel to  $\chi$ .

Instead of the individual scattering length we can introduce  $\rho(\underline{r})$ , its density distribution function.

$$\sum_j b_j \rightarrow \int \rho(\underline{r}) d^3r$$

In our case the contrast was so great with respect to the  $D_2O$  solvent that  $\rho(\underline{r})$  can be considered constant inside the molecule, and zero outside it. The  $F_{ab}(\rho^{(0)}(\underline{r}))$  and  $F_c(\rho^{(1)}(\underline{r}))$  fragments have an approximate rotational symmetry around their long axis. Let us define the body systems for the two types of fragments with the z axis being the rotational axis. We can expand  $\rho^{(i)}(\underline{r})$   $i=1,2$  in terms of the spherical harmonics

$$\rho^{(i)}(\underline{r}) = \sum_{\ell m} \rho_{\ell m}^{(i)}(\underline{r}) \varphi_{\ell m}(\theta, \phi)$$

Because of the symmetry mentioned above we have no zero terms except when  $m = 0$ .

The connection between the body systems and the space system can be established by the rotational matrices [17], [18]  $D_{mm}^{\ell}(\omega)$  which carry the space system into the body system.  $\omega$  is a short notation of the  $(\alpha, \beta, \gamma)$  Euler angles. The IgG consists of two  $F_{ab}$  fragments and one  $F_c$  fragment all of whose average relative positions are approximately known from elastic scattering studies [1].

$\omega$  is composed of three successive rotations, viz.  $\omega, \Omega, \varphi_p$ .  $\omega(t)$  gives the orientation of the molecule as a whole,  $\Omega(t)$  the distortion around the joining point if  $r(t)$  belongs to one of the  $F_{ab}$  arms,  $\Omega(t) = C$  if  $r(t)$  belongs to  $F_c$ .  $\varphi_p$  describes this T-like shape of the average relative position, so  $\frac{\pi}{2}$  for  $F_c$ ,  $\pi$  for the second  $F_{ab}$  arm.

$$e^{i\chi r_j} = \sum_{\substack{\ell, m \\ \mu_1, \mu_2}} \sqrt{4\pi(2\ell+1)} i^{\ell} j_{\ell}(\chi r) D_{0\mu_1}^{\ell}(\omega) D_{\mu_1 \mu_2}^{\ell}(\Omega) D_{\mu_2 m}^{\ell}(\varphi_p) \varphi_{\ell m}(\theta, \phi) \quad (A.4)$$

To perform the averaging we need  $P_1(\Omega_0)$ , the probability of  $\Omega_0$  at  $t=0$  and  $P(\Omega t | \Omega_0)$  the conditional probability of  $\Omega$  at  $t \neq 0$  if  $\Omega_0$  at  $t=0$ . For short time intervals we can suppose a nearly isotropic rotation which depends only

on the product  $\Omega_0^{-1}\Omega$ , and can be described by the differential equation

$$D_r \Delta_\Omega P(\Omega, t | \Omega_0) = \frac{\partial}{\partial t} P(\Omega, t | \Omega_0) \quad (\text{A.5})$$

where  $D_r$  is the rotational diffusional coefficient of the arms.  $\Delta_\Omega$  is the Laplacian. In this case [17]

$$P(\Omega, t | \Omega_0) = \sum_{\substack{\ell, \mu \\ m}} \frac{2\ell+1}{8\pi^2} D_{m\mu}^\ell(\Omega) D_{m\mu}^{\ell*}(\Omega_0) \exp(-\ell(\ell+1) D_r t) \quad (\text{A.6})$$

A similar equation describes  $P(\omega, t | \omega_0)$  with the rotational diffusional coefficient  $D_r^T$  for the whole molecule. For the sake of simplicity we suppose an equal probability on the surface of a cone of an angle  $\beta_0$  for  $P_1(\Omega_0)$ . Actually it would be enough to suppose that  $P_1(\Omega_0)$  depends only on  $\beta$  from the  $(\alpha, \beta, \gamma)$  Euler angles. For greater  $t$   $P(\Omega, t | \Omega_0)$  is not well described by (A.5) - (A.6). We have corrected this by the asymptotic behaviour  $\lim_{t \rightarrow \infty} P(\Omega, t | \Omega_0) = P_1(\Omega)$ . As there was no resultant orientation  $P_2(\omega)$  is constant on the whole spherical surface. Supposing that there is no correlation between  $\Omega(t)$  and  $\Omega_0$  when  $r(t)$  and  $r_0$  belong to different  $F_{ab}$  arms, and together with the asymptotic correction mentioned above we can calculate the expectation value. One obtains

$$\begin{aligned} \langle \chi, t \rangle = & e^{-\chi^2 D_r t} \left[ \sum_{\ell} (2\ell+1) [2A_\ell^{(0)}(\chi)]^2 \{ (1 - \langle P_\ell(\cos\beta) \rangle^2) \exp(-\ell(\ell+1) D_r t) + \right. \\ & + (1 + (-1)^\ell) \langle P_\ell(\cos\beta) \rangle^2 \} + 4A_\ell^{(0)}(\chi) A_\ell^{(1)}(\chi) \langle P_\ell(\cos\beta) \rangle P_\ell(0) + \\ & \left. + A_\ell^{(1)}(\chi)^2 \right] \exp(-\ell(\ell+1) D_r^T t) \end{aligned} \quad (\text{A.7})$$

where

$$A_\ell^{(i)}(\chi) = \int_0^a j_\ell(\chi r) \rho_\ell^{(i)}(r) r^2 dr \quad (\text{A.8})$$

$$\rho_\ell^{(i)}(r) = \sqrt{\frac{4\pi}{2\ell+1}} \rho_{\ell 0}^{(i)}(r) \quad (\text{A.9})$$

and

$$\langle P_\ell(\cos\beta) \rangle = \int P_\ell(\cos\beta) P(\Omega) d\Omega = \int_{\cos\beta_0}^1 P_\ell(\cos\beta) d(\cos\beta) / (1 - \cos\beta_0) \quad (\text{A.10})$$

Assuming that the inelasticity comes mainly from the distortion of the arms,

we can simply write 1 instead of  $\frac{-l(l+1)D_r^T t}{\dots}$ .

Supposing a rigid molecule  $\cos\beta_0 = 1$  or  $\langle P_l(\cos\beta) \rangle = 1$ , then

$$| (X,t) = e^{-X^2 D_r t} \sum_l (2l+1) [2A_l^{(0)}(X)^2 (1+(-1)^l) + 4A_l^{(0)}(X) A_l^{(1)}(X) P_l(0) + A_l^{(1)}(X)^2] \exp(-l(l+1) D_r^T t) \quad (A.11)$$

Table I. Correlation time (in nsec) obtained from different sources and normalized to the viscosity of 7.33 w% IgG solution in D<sub>2</sub>O

	$\tau_r = \frac{1}{D_r} r$	$\tau = \frac{1}{D_r}$
1. Rigid model	1700	-
2. Flexible model ( $\beta_{\max} = 20^\circ$ )	-	520
3. Flexible model ( $\beta_{\max} = 50^\circ$ )	-	900
4. Estimation by formula	6000	-
5. Wobbling time according to (5)	-	1050

Table II. Dependence of the relative shortening of the average distance in % between the tips of the Fab arms as a function of  $\beta_{\max}$

$\beta_{\max}$ (degrees)	$\Delta l/l$ (%)
10	0.3
20	1.6
30	3.4
40	5.1
50	8.2

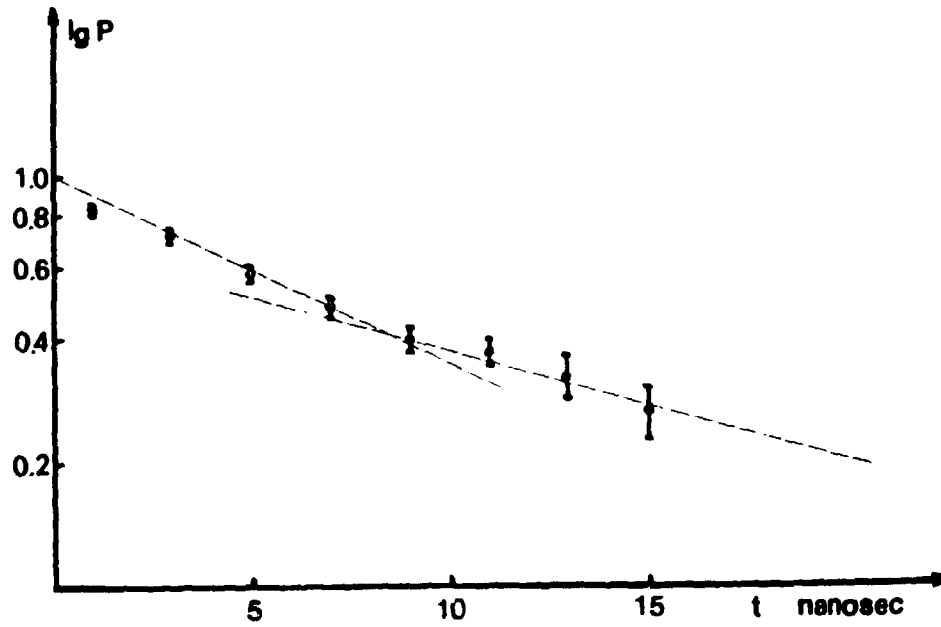


Fig. 1. Logarithm of spin-echo signal versus time ( $\chi = 1,53 \text{ nm}^{-1}$ )

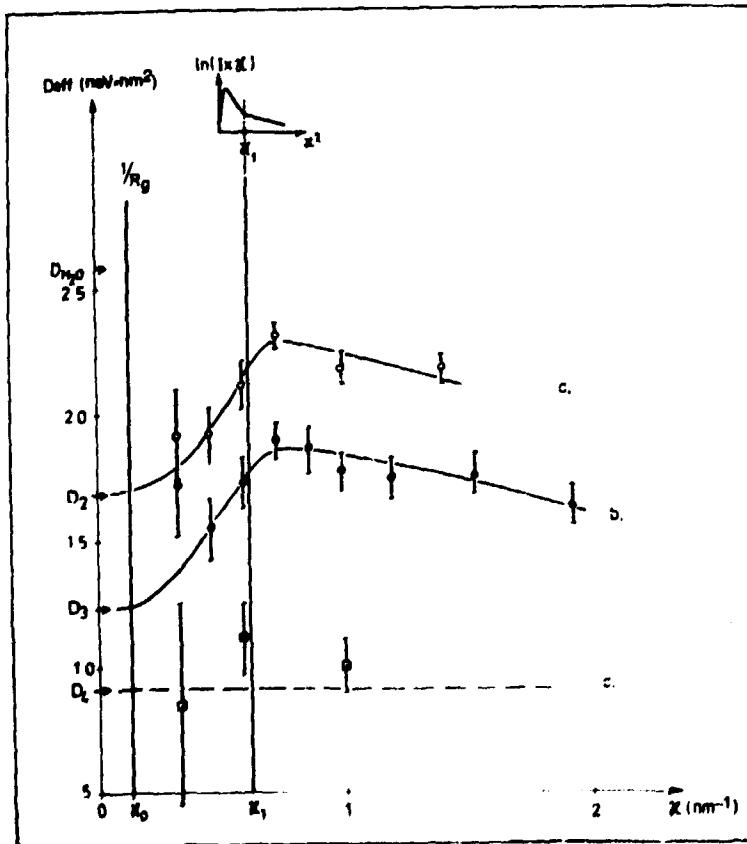


Fig. 2.

Experimental values of  $D_{\text{eff}}$  as a function of  $\chi$ .

a - 3.67 w% IgG in  $D_2O$ ;

b - 7.33 w% IgG in  $D_2O$ ;

c - 7.33 w% IgG + 18 w% sucrose in  $D_2O$   $\chi_0 = 1/R_g$ .

$\chi_1$  - corresponds to the cross-section of the two straight-line parts on the small-angle scattering intensity distribution given in Porod coordinates [3] (see insert).  $D_{H_2O}$  - diffusion constant of human IgG [16];

$D_2$ ,  $D_3$  and  $D_4$  stand for the translational diffusion constant for curves a) b) and c) respectively. The continuous and broken lines are for guidance only.

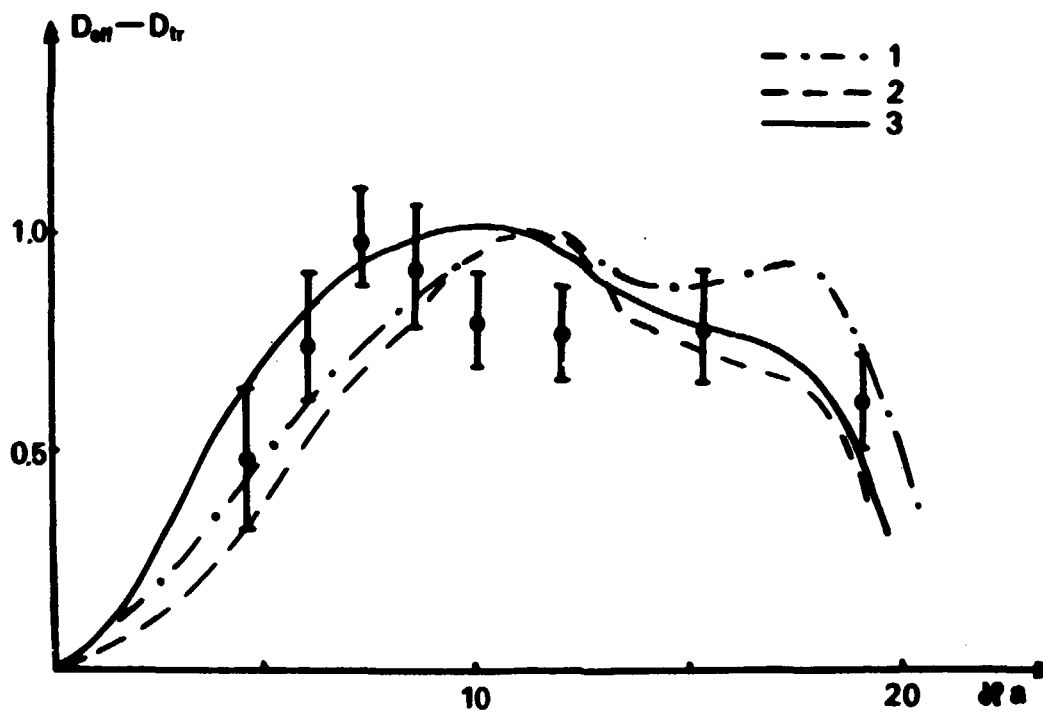


Fig. 3. Calculated  $D_{\text{eff}}^{(c)} - D_{\text{tr}}$  curves for typical models in dimensionless coordinates. 1 - rigid model; 2- flexible model ( $\beta_{\text{max}} = 20^\circ$ ); 3 - flexible model ( $\beta_{\text{max}} = 50^\circ$ );  $a = 10 \text{ nm}$

## REFERENCES

- [1] L. Cser, I.A. Gladkih, F. Franek - Yu.M. Ostanovich: *Colloid and Polymer Sci.* 259, 625-640 (1981)
- [2] J. Deisenhofer, P.M. Colman, R. Huber, M. Haupt, G. Schwick: *Hoppe-Seyler's Z. Biol. Chem.* 357, 435 (1976)
- [3] L. Cser, F. Franek, I.A. Gladkih, A.B. Kunchenko, Yu.M. Ostanovich: *Eur. J. Biochem.* 116, 109-116 (1981)
- [4] J. Yguerabide, H.F. Epstein, L. Stryer: *J. Mol. Biol.* 51, 753-590 (1970)
- [5] D.C. Hanson, J. Yguerabide, V.N. Schumaker: *Biochemistry* 20, 6842-6852 (1981)
- [6] F. Franek, L. Simek: *Eur. J. Immunol.* 1, 300-302 (1971)
- [7] F. Franek, J. Doskocil, L. Simek: *Immunochemistry* 11, 803-809 (1974)
- [8] F. Franek: *FEBS Symp.* 36, 63-75 (1975)
- [9] F. Franek, Z. Odsovska, L. Simek: *Eur. J. Immunol.* 9, 976-701 (1979)
- [10] L. Cser, F. Franek, I.A. Gladkih, R.S. Nezlin, J. Novotny, Yu.M. Ostanovich: *FEBS Letters* 80, 329-331 (1977)
- [11] F. Mezei: In *Neutron Spin Echo*, ed. by F. Mezei: *Lecture Notes in Physics*, Vol. 128 (Springer Verlag, Heidelberg, 1980) p.3
- [12] P.A. Dalgiesh, J.B. Hayter, F. Mezei: *ibid.* p.66
- [13] *CRC Handbook of Biochemistry and Mol. Biology, Proteins*, Vol. II. ed. by G.D. Fasman Ph.D. 3rd edition, CRC Press Inc. Cleveland 1976. p.249
- [14] L.K. Nicholson, J.S. Higgins, J.B. Hayter: in *Neutron Spin Echo*, *ibid.* p.75-80
- [15] R.C. Valentine, N.M. Green: *J. Mol. Biol.* 27, 615 (1967)
- [16] F. Volino: *Proc. of NATO Adv. Stud. ser.B. phys.* 33, 233 (1977)
- [17] V.F. Sears: *Canad. J. of Phys.* 45, 237 (1967)
- [18] O.M. Brink, G.R. Sathler: *Angular Momentum*, Oxford Libr. (1971)

Kiadja a Központi Fizikai Kutató Intézet  
Felelős kiadó: Kroó Norbert  
Szakmai lektor: Sváb Erzsébet  
Nyelvi lektor: Harvey Shenker  
Gépelte: Simándi Józsefné  
Példányszám: 180      Törzsszám: 82-668  
Készült a KFKI sokszorosító üzemében  
Felelős vezető: Nagy Károly  
Budapest, 1982. december hó